Available online at www.sciencedirect.com
SCIENCE DIRECT®
Journal of Magnetic Resonance 169 (2004) 13–18
JMR Journal of Magnetic Resonance
www.elsevier.com/locate/jmr

High-resolution NMR of static samples by rotation of the magnetic field

Carlos A. Meriles,[a,b] Dimitris Sakellariou,[a,b] Adam Moulé,[a,b] Maurice Goldman,[c] Thomas F. Budinger,[b] and Alexander Pines[a,b,*]

[a] *Department of Chemistry, Materials Sciences Division, University of California, Berkeley, CA 94720, USA*
[b] *Ernest Orlando Lawrence Berkeley National Laboratory, Berkeley, CA 94720, USA*
[c] *CEA, Saclay, DSM/DRECAM/Service de Physique de l'Etat Condensé, F-91191 Gif sur Yvette cedex, France*

Received 21 January 2004; revised 24 March 2004
Available online 27 April 2004

Abstract

Mechanical rotation of a sample at 54.7° with respect to the static magnetic field, so-called magic-angle spinning (MAS), is currently a routine procedure in nuclear magnetic resonance (NMR). The technique enhances the spectral resolution by averaging away anisotropic spin interactions thereby producing isotropic-like spectra with resolved chemical shifts and scalar couplings. It should be possible to induce similar effects in a static sample if the direction of the magnetic field is varied, e.g., magic-angle rotation of the B_0 field (B_0-MAS). Here, this principle is experimentally demonstrated in a static sample of solid hyperpolarized xenon at ~3.4 mT. By extension to moderately high fields, it is possible to foresee interesting applications in situations where physical manipulation of the sample is inconvenient or impossible. Such situations are expected to arise in many cases from materials to biomedicine and are particularly relevant to the novel approach of ex situ NMR spectroscopy and imaging.

Keywords: Rotating field; Magic angle field rotation; B0-MAS; High-resolution; Hyperpolarized xenon; Coherent averaging; Field spinning

The versatility of magnetic resonance spectroscopy derives from its ability to manipulate interactions that quite often obscure the desired information. Examples abound in solid state NMR where varied sources of line broadening in the spectrum are removed (and/or reintroduced). Central to this methodology is the sample rotation around an axis at 54.7° with respect to the static field direction, a technique known as magic angle spinning (MAS). Shortly, after the method was introduced [1,2], Andrew and Eades [3] suggested that identical results could be obtained if rather than spinning the sample, the field direction was rotated about an axis inclined at the magic angle. This idea has been analyzed and extended to generalized field trajectories [4] and pulse sequences within the context of Zero-Field NMR and dipolar time-reversal echoes [5]. A more recent implementation has been used to study Berry's phase after a 2π-rotation of the field and has led to the development of a NMR-based gyroscope [6]. Field rotation at the magic angle has also been combined with field cycling to study the dynamics of liquid crystals [7].

To gain spectral resolution in heterogeneous and anisotropic samples, this approach becomes potentially useful for situations where mechanical manipulation of the sample is inconvenient or impossible. An important example is in vivo NMR where susceptibility broadening often prevents the acquisition of highly resolved spectra [8]. This limitation has prompted the use of methods that synchronize a radiofrequency pulsing scheme with an ultraslow rotation of the living subject [9]. Unfortunately, spin relaxation prevents the use of spinning rates lower than ~1 Hz and, despite a remarkable resolution improvement, the method proves inadequate in many practical situations, in particular, for large subjects such as human beings.

In a somewhat different context, field rotation could also be used in combination with ex situ NMR

* Corresponding author. Fax: 1-510-486-5744.
E-mail address: Pines@cchem.berkeley.edu (A. Pines).

1090-7807/$ - see front matter © 2004 Elsevier Inc. All rights reserved.
doi:10.1016/j.jmr.2004.03.023

spectroscopy where, by definition, a static extended sample placed beyond the physical confines of the magnet is to be analyzed [10]. A potential application is oil well-logging [11] where paramagnetic impurities on the walls of the rock pores lead to strong broadening [12] or human proton spectroscopy of membrane components which are obscured by anisotropic susceptibilities. In this article, we will first review how field spinning affects different spin interactions. Then, we will experimentally illustrate this methodology with an example and we will finally discuss its implementation at higher fields.

Consider an ensemble of interacting spins I_j in the presence of a strong time dependent magnetic field $\Omega_0(t)$ (in this article, we take the spin gyromagnetic ratio equal to one). The system spin density operator $\rho(t)$ evolves according to the Liouville equation $\mathrm{d}\rho(t)/\mathrm{dt} = -i[H(t), \rho(t)]$, where $H(t)$ represents the system Hamiltonian given by

$$\begin{aligned} H(t) &= H_{\mathrm{Z}} + H_{\mathrm{S}} + H_{\mathrm{D}} \\ &= \sum_j \vec{I}_j \cdot \vec{\Omega}_0(t) + \sum_j \vec{I}_j \cdot \overleftrightarrow{S} \cdot \vec{\Omega}_0(t) + \sum_{i,j} \vec{I}_i \cdot \overleftrightarrow{D}_{ij} \cdot \vec{I}_j, \end{aligned} \tag{1}$$

where H_{Z} represents the Zeeman interaction between the nuclear spin and the time dependent magnetic field whereas H_{S} takes into account local electronic contributions and H_{D} represents all bilinear contributions to the Hamiltonian derived from inter-spin interactions. We will refer to $\overleftrightarrow{S}$ as the chemical shift tensor, but variations of the local magnetic field due to susceptibility or Knight shifts can also be included here when necessary. For brevity, we will focus on dipolar interactions although quadrupolar or J-interactions can be included with only minor formal changes [13].

For simplicity, let us assume that the field has constant amplitude Ω_0 and that it precesses at a constant rate Ω_r about the laboratory z-axis at a fixed angle θ. Transforming to the precessing reference frame where the magnetic field looks static (and vertical), we now define the transformed spin density operator

$$\tilde{\rho}(t) = \mathrm{e}^{i\tilde{\theta}I_y}\mathrm{e}^{i\Omega_r t I_z}\rho(t)\mathrm{e}^{-i\Omega_r t I_z}\mathrm{e}^{-i\tilde{\theta}I_y}, \tag{2}$$

where $\tan(\tilde{\theta}) = \Omega_0 \sin(\theta)/(\Omega_0 \cos(\theta) - \Omega_r)$. Upon substitution in the Liouville equation, we get

$$\frac{\mathrm{d}\tilde{\rho}(t)}{\mathrm{dt}} = -i\Big[\Omega_{\mathrm{eff}} I_z + \mathrm{e}^{i\tilde{\theta}I_y}\mathrm{e}^{i\Omega_r t I_z}(H_{\mathrm{S}} + H_{\mathrm{D}})\mathrm{e}^{-i\Omega_r t I_z}\mathrm{e}^{-i\tilde{\theta}I_y}, \tilde{\rho}(t)\Big], \tag{3}$$

with $\Omega_{\mathrm{eff}}^2 = \Omega_0^2 + \Omega_r^2 - 2\Omega_r\Omega_0\cos(\theta)$. In Eq. (3), the evolution of the density operator is governed by a static magnetic field of amplitude Ω_{eff} in the presence of a time-modulated chemical shift and dipolar interactions. The effective dependence that results from this modulation is obtained by expanding H_{S} and H_{D} in spherical tensor components and by using Wigner relations to calculate rotations in spin space. In contrast to H_{D}, the chemical shift Hamiltonian H_{S} depends on the magnetic field and, for this reason, it is better to treat each case separately. Regrouping terms in the expression for H_{S}, we write $H_{\mathrm{S}} = \sum_{q=-1}^{1}(-1)^q A_{1q} T_{1-q}$, where $A_{10} = \left(\overleftrightarrow{S}\cdot\vec{\Omega}_0\right)_z$, etc as defined in ref. (13). After a lengthy but straightforward calculation, we obtain

$$\begin{aligned} (H_{\mathrm{S}})_{\mathrm{eff}} \equiv \mathrm{e}^{i\tilde{\theta}I_y}\mathrm{e}^{i\Omega_r t I_z} H_{\mathrm{S}} \mathrm{e}^{-i\Omega_r t I_z}\mathrm{e}^{-i\tilde{\theta}I_y} \cong \Omega_0 I_z \Bigg\{ \sigma_{\mathrm{iso}} \cos\left(\tilde{\theta} - \theta\right) \\ + \frac{1}{2}\sqrt{\frac{2}{3}}\sigma_{20}\Big(3\cos\tilde{\theta}\cos\theta - \cos\left(\tilde{\theta} - \theta\right)\Big)\Bigg\}, \end{aligned} \tag{4}$$

where $\sigma_{\mathrm{iso}} = \frac{1}{3}\mathrm{T_r}\left\{\overleftrightarrow{S}\right\}$ represents the isotropic (generalized) chemical shift and $\sigma_{20} = \frac{1}{\sqrt{6}}\left(3S_{zz} - \mathrm{T_r}\left\{\overleftrightarrow{S}\right\}\right)$. In Eq. (4), terms not commuting with I_z have not been included (secular approximation). On the other hand, Ω_r has been chosen to be larger than $\|H_{\mathrm{S}}\|$, the magnitude of the interaction. This makes it possible to also disregard time dependent contributions because they average out over the time scale of the spin evolution. Eq. (4) shows that a simple rotation of the field about a cone leads to a scaling of both the isotropic and the anisotropic part of the chemical shift. As expected, the scaling factors are different for each case and are given by

$$\Lambda_{\mathrm{SI}} = \cos(\tilde{\theta} - \theta) = \left(1 + \cos\tilde{\theta}\frac{\Omega_r}{\Omega_{\mathrm{eff}}}\right)\frac{\Omega_{\mathrm{eff}}}{\Omega_0}, \tag{5}$$

$$\begin{aligned} \Lambda_{\mathrm{SA}} &= \frac{1}{2}\Big(3\cos\tilde{\theta}\cos\theta - \cos(\tilde{\theta} - \theta)\Big) \\ &= \frac{1}{\Omega_0}\left(\frac{1}{2}\Omega_{\mathrm{eff}}\Big(3\cos^2\tilde{\theta} - 1\Big) + \Omega_r\cos\tilde{\theta}\right). \end{aligned} \tag{6}$$

In the limit of adiabatic rotation ($\Omega_r << \Omega_{\mathrm{eff}}$), the isotropic part remains unscaled whereas the anisotropic contribution can be cancelled out by choosing $\tilde{\theta}$ to be the magic angle. Because in this limit $\tilde{\theta} \approx \theta$, this corresponds to the case in which the field trajectory describes a cone of approximately 55 degrees [14].

Because H_{D} is independent of the magnetic field, its treatment is straightforward. As usual [13], we expand the dipolar interaction into its irreducible spherical tensor components $H_{\mathrm{D}} = \sum_{y=-2}^{2}(-1)^q A_{2q} T_{2-q}$. After applying Wigner relations for rotations in spin space, we obtain

$$(H_{\mathrm{D}})_{\mathrm{eff}} \equiv e^{i\tilde{\theta}I_y} e^{i\Omega_r t I_z} H_{\mathrm{D}} e^{-i\Omega_r t I_z} e^{-i\tilde{\theta}I_y} = \frac{1}{2}\Big(3\cos^2\tilde{\theta} - 1\Big)A_{20}T_{20}, \tag{7}$$

where, as before, we have assumed the limit of fast rotation and we have disregarded terms not commuting with the Zeeman Hamiltonian.

Eq. (7) shows that the dipolar interaction can be removed from the spectrum if only a small field component $\Omega_\perp = \Omega_0 \sin\theta$ is applied at a frequency Ω_r slightly

off-resonance with respect to the static field component $\Omega_{//} = \Omega_0 \cos\theta$. This case, with $\theta << 1$, corresponds to the Lee-Goldburg condition for homonuclear dipolar decoupling [15] and according to Eq. (5), leads to a scaling of the isotropic chemical shift $\Lambda_{SI} \approx 1/\sqrt{3}$. In this limit, the same holds true for the anisotropic contribution, which, in general, cannot be removed if only rf irradiation at high field is used.

An example of a field-rotation scheme designed to average out anisotropic interactions in a static sample is described below. In this particular case, field spinning is used to remove the dipolar broadening from a spectrum of solid hyperpolarized ^{129}Xe. Fig. 1 shows the experimental setup. A gas mixture containing xenon was continuously circulated along a closed loop. Xenon hyperpolarization was induced by contact with Rb gas confined by cold traps to a hot glass cell at ~160 °C. Rb electronic hyperpolarization was induced in a field of ~20 G by a circularly polarized 50 W laser operating at 795 nm. Experimental details regarding this homebuilt system, the procedure and the mixture composition can be found elsewhere [16].

The insert in Fig. 1 describes the array at the detection site. Three orthogonal Helmholtz pairs are used to set the field direction. Throughout the experiment one of the pairs provided a constant field of ~21 G. The other two pairs were driven via two 600 W homebuilt current amplifiers. A high-Q coil for excitation and detection of the NMR signal surrounded a glass cell connected to the gas loop. The probe was contained inside a long cylindrical dewar in which the temperature was controlled by a system that alternated pre-cooled and room temperature nitrogen.

^{129}Xe magnetic resonance at 24 kHz was carried out by using a homebuilt spectrometer based on a Tecmag-Orion console for audiofrequency control, field manipulation and data acquisition. A two-channel Hewlett-Packard (3326A) frequency synthesizer simultaneously provided 10 $V_{p\text{-}p}$ audiofrequency for excitation and 0.5 $V_{p\text{-}p}$ as a phase reference. Quadrature detection was accomplished by a Stanford Research SR830-DSP lock-in amplifier preceded by a Stanford Research SR560 preamp for signal enhancement and pre-filtering. A tank circuit tuned to resonance was used

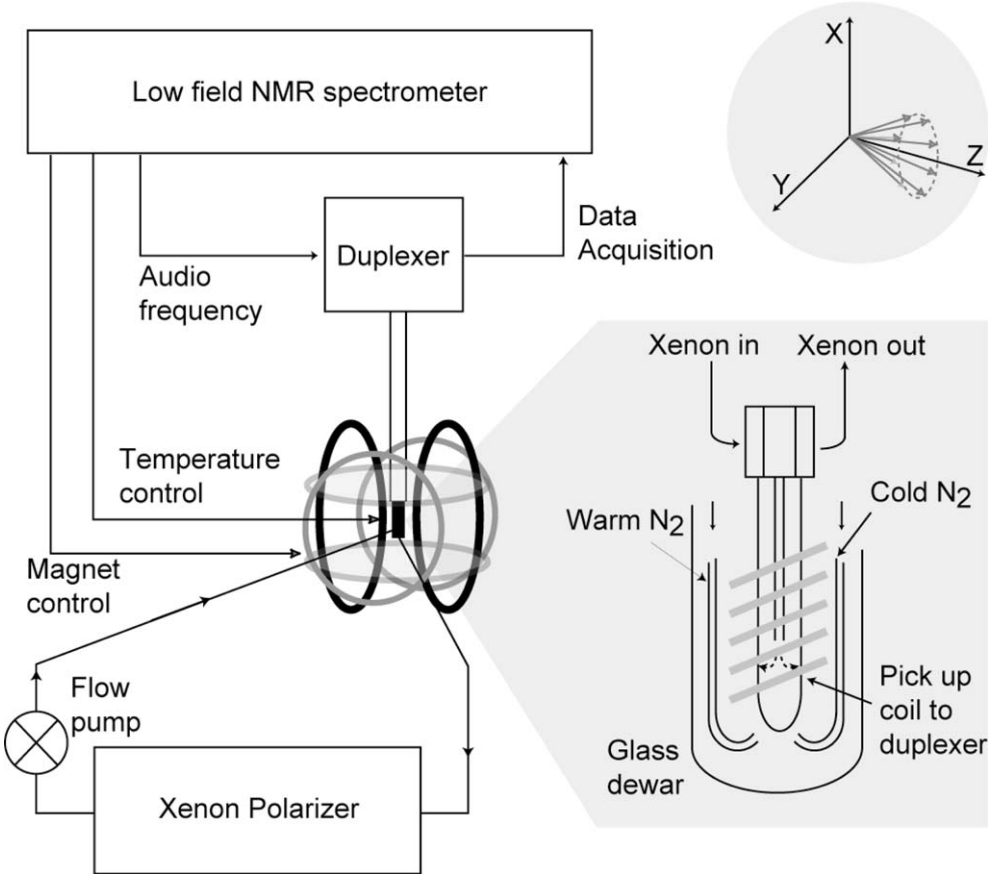

Fig. 1. Schematics of the experimental setup. A closed circuit xenon polarizer pumps the gas mixture through a solenoidal pick up coil in a low frequency NMR spectrometer. The magnetic field direction at the detection site can be varied by a set of three mutually orthogonal Helmholtz pairs controlled by the spectrometer console. Xenon can be removed from the gas mixture by condensing it within the sensitive volume by inletting cold nitrogen. For this purpose, a ~40 cm long glass dewar surrounds the sample probe. The Xe gas is reintroduced to the mixture by using room temperature N_2 gas. The field component along Z (not displayed) remains constant at all times.

to excite and pick up the spin signal. The duplexer was homebuilt and the isolation was provided by a combination of digital gates and mechanical relays. Due to the high Q of the coil, a damping circuit acting after pulse excitation was added to reduce the spectrometer dead time to 500 μs.

To avoid saturating the receiver, we implemented a 2D scheme that indirectly probes the evolution of the magnetization while the field direction changes (see Fig. 2). The resulting 2D spectrum is shown in Fig. 3. In the direct dimension F_2, the spectrum displays the full dipolar broadening of solid ^{129}Xe, which is ~350 Hz as expected [17]. To a large extent, this is removed by magic angle field spinning: the linewidth in the F_1 dimension has narrowed down to ~60 Hz, approximately 1/6 of the original. Notice the absence of sidebands in the isotropic spectrum due to the synchronization of data acquisition and spinning rate. Also notice that because the field magnitude is larger during t_1, the actual resonance frequency in the evolution period shifts to about 40 kHz. Since the carrier frequency remains unaltered, the detected signal folds several times over the narrow spectral window in F_1.

Several experimental limitations may account for the observed residual broadening of the isotropic spectrum. Imperfections due to the non-linear behavior of the current amplifiers during the zero-current crossings and uncompensated geometrical differences between the X and Y coil set, cause the field trajectory to depart from the ideal one and lead to undesired broadening of the isotropic peak. Other sources of broadening are the finite time spent in tilting the field direction prior to acquisition and field inhomogeneities. This last contribution, measured to be 500 ppm at the sample site, accounts for 20 Hz at ~34 G (the net field amplitude during t_1) [18].

Work is underway to reduce all the above imperfections to a minimum and more efficient field trajectories are being developed to optimize the ultimate attainable resolution. For example, symmetrized field trajectories could be used to eliminate dipolar broadening to first as well as to higher orders in the average Hamiltonian expansion [19]. Field trajectories that only sample a limited number of points over the rotation cone [4] are also a possibility that could allow for a direct detection during the field evolution. This field trajectory could be chosen to emulate double angle rotation (DOR) [20] to eliminate up to second order quadrupolar broadening or could be combined with synchronized radiofrequency pulses in a magic angle hopping (MAH) [21] type approach. This last possibility is particularly interesting

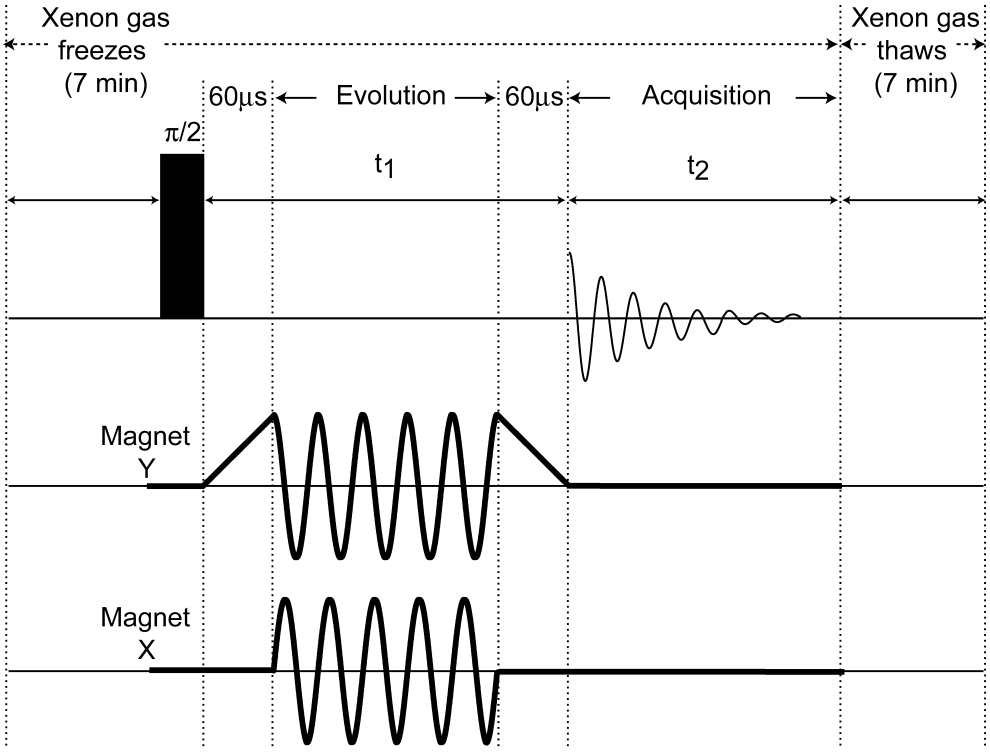

Fig. 2. The diagram describes the protocol used in our experiment. During the first few minutes, cold nitrogen is blown close to the pick up coil condensing at this point most of the xenon gas in the mixture. Evolution under field spinning starts after the sample has been excited and the field direction has been adiabatically readjusted (magnet along X is on). At the end of the evolution time t_1, all lateral components are switched off and data acquisition is carried out. Warmer nitrogen finally leads to sample thawing and repolarization of the xenon gas. The procedure is then repeated for a different t_1.

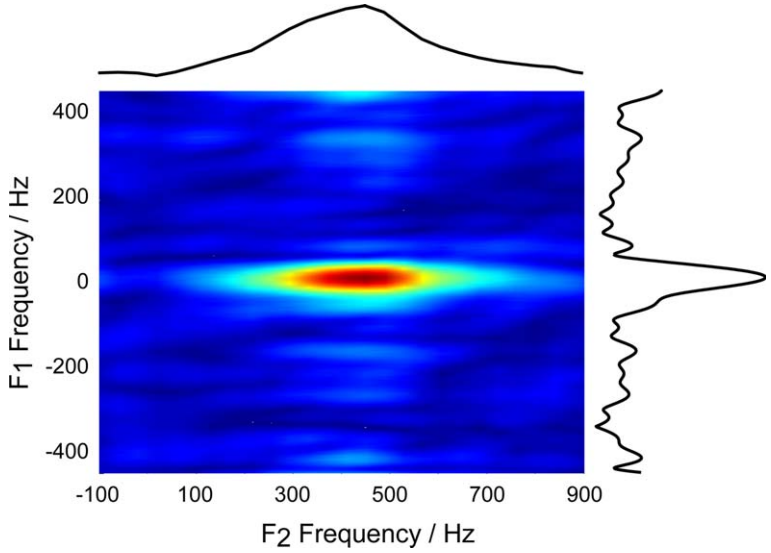

Fig. 3. Dipolar—isotropic chemical shift correlation spectrum in a static sample of hyperpolarized solid xenon obtained by field rotation at the magic angle. The acquisition dimension F_2 (plotted horizontally) displays the full dipolar broadening observed when the field remains static (FWHM ~350 Hz). This broadening is substantially reduced during the evolution dimension F_1 (plotted vertically) by making the field describe a conical trajectory at the magic angle prior to acquisition. In this case, the projection along F_1 exhibits a residual broadening of only ~60 Hz largely due to experimental imperfections (see text). The field strength was ~34 G during field spinning and was reduced to ~21 G during acquisition. The number of increments in the indirect dimension was 32 in steps of 1 ms and the dwell time during acquisition was 200 μs. Two scans were averaged for each evolution time. The excitation pulse was 200 μs long. The field-spinning rate was 2 kHz. Notice the absence of sidebands in the narrowed spectrum due to the rotor synchronization imposed by the chosen sampling time (two rotations per point in the indirect dimension).

because it may enable the use of ultraslow spinning rates that have been successfully used to remove susceptibility broadening in samples of biological tissue [9]. Finally, generalized field trajectories could be used to detect isotropic–anisotropic spectral correlations in a way similar to switched angle spinning (SAS) [22,23]. Notice that because the field (direction) changes during acquisition, our experiment provides an elementary example of such correlations.

Crucial for all these applications in a practical setting is the use of a stronger magnetic field, a condition that necessarily renders the technique demanding beyond fractions of a Tesla. However, the practical limits of the ultimately attainable field magnitude still remain to be set. Magic angle rotation could benefit from the rich variety of instruments and optimization procedures developed for fast field cycling spectroscopy. In particular, if only a ~1 Hz rotation rate is used to remove susceptibility broadening, the technical requirements on a field of ~1 T are far less demanding than those currently standard in field cycling.

Other strategies can also be used to further mitigate the technical constraints. It has been demonstrated recently [24] that a scaled isotropic chemical shift spectrum can be obtained if the field alternatively moves over two cones, each with an angle smaller than the magic angle. The procedure will permit having less intense X and Y field components at the expense of a slower chemical shift evolution, a convenient trade-off given the dependence of the overall power on the spinning angle.

As suggested by Andrew and Eades 40 years ago, field rotation can be used to remove anisotropic broadening from the NMR spectrum. In this article we have revisited this concept and formally shown the conditions that the field trajectory must fulfill depending on the type of anisotropy to be removed. We have illustrated these principles experimentally by averaging out the dipolar broadening from the NMR spectrum of hyperpolarized solid ^{129}Xe. An extension of the procedure to remove chemical shift and magnetic susceptibility anisotropies is straightforward and may prove useful in brain, liver or heart in vivo spectroscopy or for rocks and other porous, and heterogeneous materials to cite a few examples. Technical requirements may become demanding at high fields, but the procedure presented here can be combined with other methods that extract high-resolution information either off the magic angle or at an ultraslow rotation rate. For the latter case, a mechanical rotation of the magnet (or part of it) is also a possibility that could be employed when strong permanent magnets are used as the field source.

Acknowledgments

We gratefully acknowledge E. Granlund and W.M. Chan for their assistance with hardware and instrumentation. This work was supported by the Director, Office of Science, Office of Basic Energy Sciences, Materials Sciences and Engineering Division, of the US

Department of Energy under Contract No. DE-AC03-76SF00098.

References

[1] E.R. Andrew, A. Bradbury, R.G. Eades, Nuclear magnetic resonance spectra from a crystal rotated at high speed, Nature 182 (1958) 1659.

[2] I.J. Lowe, Free induction decays of rotating solids, Phys. Rev. Lett. 2 (1959) 285.

[3] E.R. Andrew, R.G. Eades, Possibilities for high-resolution nuclear magnetic resonance spectra of crystals, Disc. Farad. Soc. 34 (1962) 38.

[4] C.J. Lee, D. Suter, A. Pines, Theory of multiple-pulse NMR at low and zero fields, J. Magn. Reson. 75 (1987) 110.

[5] A. Llor, Z. Olejniczak, J. Sachleben, A. Pines, Scaling and time reversal of spin couplings in zero-field NMR, Phys. Rev. Lett. 67 (1991) 1989; A. Llor, Z. Olejniczak, A. Pines, Coherent isotropic averaging in zero-field nuclear magnetic resonance. I. General theory and icosahedral sequences, J. Chem. Phys. 103 (1995) 3966; Coherent isotropic averaging in zero-field nuclear magnetic resonance. II. Cubic sequences and time-reversal of spin couplings, J. Chem. Phys. 103 (1995) 3982.

[6] P. Härle, G. Wäckerle, M. Mehring, A nuclear-spin based rotation sensor using optical polarization and detection methods, Appl. Magn. Reson. 5 (1993) 207.

[7] F. Noack, St. Becker, J. Struppe, Applications of field-cycling NMR, Annu. Rep. NMR Spectros. 33 (1997) 1.

[8] L.L. Cheng, M.J. Ma, L. Becerra, T. Ptak, I. Tracey, A. Lackner, R.G. González, Quantitative neuropathology by high resolution magic angle spinning proton magnetic resonance spectroscopy, Proc. Natl. Acad. Sci. USA 94 (1997) 6408.

[9] J.Z. Hu, D.N. Rommereim, R.A. Wind, High-resolution ^{1}H NMR spectroscopy in rat liver using magic angle turning at a 1 Hz spinning rate, Magn. Reson. Med. 47 (2002) 829.

[10] C.A. Meriles, D. Sakellariou, H. Heise, A. Moulé, A. Pines, Approach to high-resolution ex situ NMR spectroscopy, Science 293 (2001) 82.

[11] T.M. Brill, S. Ryu, R. Gaylor, J. Jundt, D.D. Griffin, Y.Q. Song, P.N. Sen, M.D. Hürlimann, Nonresonant multiple spin echoes, Science 297 (2002) 369.

[12] C.A. Meriles, D. Sakellariou, A. Pines, Resolved magic-angle spinning of anisotropic samples in inhomogeneous fields, Chem. Phys. Lett. 358 (2002) 391.

[13] M. Mehring, Principles of High Resolution NMR in Solids, Springer-Verlag, Berlin, 1983.

[14] A simple calculation shows that, in the general case, Λ_{SA} can be made exactly zero only if the field components parallel and perpendicular to the axis of rotation are chosen to satisfy $\Omega_{//}^2 = \Omega_r^2 + 2\Omega_\perp^2$.

[15] W.I. Goldburg, M. Lee, Nuclear-magnetic-resonance line narrowing by a rotating RF field, Phys. Rev. Lett. 11 (1963) 255.

[16] A. Wong-Foy, S. Saxena, A.J. Moulé, H.L. Bitter, J.A. Seeley, R. McDermott, J. Clarke, A. Pines, Laser-polarized ^{129}Xe NMR and MRI at ultralow magnetic field, J. Magn. Reson. 157 (2002) 235.

[17] D.M. TonThat, M. Ziegeweid, Y.-Q. Song, E.J. Munson, S. Appelt, A. Pines, J. Clarke, SQUID detected NMR of laser-polarized xenon at 4.2 K and at frequencies down to 200 Hz, Chem. Phys. Lett. 272 (1997) 245.

[18] Since the spin evolution during field spinning is probed indirectly, the sample had to be thawed, repolarized and refrozen for each scan. In this procedure the repeatability of the signal amplitude is crucial. This was improved by the use of a closed circuit with a fixed amount of xenon.

[19] U. Haeberlen, J.S. Waugh, Coherent averaging effects in magnetic resonance, Phys. Rev. 175 (1968) 453.

[20] B.F. Chmelka, K.T. Mueller, A. Pines, J. Stebbins, Y. Wu, J.W. Swanziger, O-17 NMR in solids by dynamic-angle spinning and double rotation, Nature 339 (1989) 42.

[21] N.M. Szeverenyi, A. Bax, G.E. Maciel, Magic-angle hopping as an alternative to magic-angle spinning for solid state NMR, J. Magn. Reson. 61 (1985) 440.

[22] A. Bax, N.M. Szeverenyi, G.E. Maciel, Chemical shift anisotropy in powdered solids studied by {2D} {FT} {NMR} with flipping of the spinning axis, J. Magn. Reson. 55 (1983) 494.

[23] T. Terao, T. Fujii, T. Onodera, A. Saika, Switching-angle sample-spinning NMR spectroscopy for obtaining powder-pattern-resolved 2D spectra: measurements of ^{13}C chemical-shift anisotropies in powdered 3,4-dimethoxybenzaldehyde, Chem. Phys. Lett. 107 (1984) 145.

[24] D. Sakellariou, C.A. Meriles, R. Martin, A. Pines, High-resolution NMR of anisotropic samples with spinning away from the magic angle, Chem. Phys. Lett. 377 (2003) 333.